

Nonanalytic behaviour in a log-normal Markov functional model

Dan Pirjol

In a previous paper it was shown that a Markov-functional model with log-normally distributed rates in the terminal measure displays nonanalytic behaviour as a function of the volatility, which is similar to a phase transition in condensed matter physics. More precisely, certain expectation values have discontinuous derivatives with respect to the volatility at a certain critical value of the volatility. Here we discuss the implications of these results for the pricing of interest rates derivatives. We point out the presence of nonanalyticity effects in other quantities of the model, focusing on the properties of the Libor probability distribution function in a measure in which it is simply related to caplet prices. We show that the moments of this distribution function have nonanalytic dependence on the volatility, which are also similar to a phase transition. We study in some detail the pricing of caplets on Libor rates and Libor payments in arrears, and show that the convexity adjustment for the latter is also nonanalytic in the model volatility.

I. INTRODUCTION

An important class of interest rate models, which includes many of the models currently used in practice, is the class of Markov-functional models [1–4]. The advantage of these models is that the prices of zero coupon bonds can be expressed as a functional of a low-dimensional Markov process. The specification of this functional dependence allows one to model the distribution of the forward rates with a prescribed implied volatility smile, such that these models can be calibrated exactly to a set of market instruments, such as swaptions or caplets. They are particular cases of short rate models in discrete or continuous time [5–12].

We consider a one-dimensional Markov-functional model with log-normally distributed rates in the forward terminal measure. In Ref. [13] it was shown that this model can be solved exactly for the time-homogeneous case of constant volatility. Exact results can be found for the dependence of all zero coupon bonds on the Markovian driver.

The exact solution of the model was used in [13] to study its behavior as a function of volatility. The main results can be summarized as follows: the model has two distinct limiting regimes, at low and large volatility, respectively, with very different qualitative behaviour. These regimes are separated by a sharp transition, occurring at a critical value of the volatility, which resembles a first order phase transition in condensed matter physics. Certain expectation values of dynamical quantities are nonanalytic at the critical volatility, and have discontinuous derivatives with respect to the volatility.

In this paper we study further the behaviour of the model around the critical point, focusing on the properties of the Libor distribution function. The shape of the Libor distribution function, in a measure in which it is simply related to caplet prices (the forward measure), changes suddenly above the critical volatility, and becomes very concentrated at small values of the Libor rates in addition to forming a long tail. This phenomenon

is reflected in the behaviour of the Black caplet volatility, which undergoes a sudden change at the critical volatility. While for subcritical volatility the caplet smile is flat to a good approximation, and it is equal to the Libor volatility, above the critical volatility the ATM caplet implied volatility increases suddenly, and a nontrivial caplet smile appears. We show that the first few moments of the Libor distribution function have nonanalyticity points as functions of the volatility, similar to phase transitions. This leads to nonanalyticity in the caplet prices and caplet Black volatility, and suggests that the presence of non-analyticity in volatility is a generic feature of models with log-normal rates in the terminal measure.

II. THE MODEL

We consider a Markov functional model with discrete time evolution. The model is defined on a finite set of dates

$$0 = t_0 < t_1 < \dots < t_n \quad (1)$$

Usually the t_i are equally spaced, e.g. by 3 or 6 months apart, but we will keep them completely general, and denote $\tau_i \equiv t_{i+1} - t_i$.

The fundamental dynamical quantities are the zero coupon bonds $P_{i,j} \equiv P_{t_i,t_j}$, which are functions of a one-dimensional Markov process $x(t)$, which will be assumed to be a simple Wiener process. The model is defined by the probability distribution of the Libor rates $L_i = \tau_i^{-1}(P_{i,i+1}^{-1} - 1)$ for the (t_i, t_{i+1}) period. The Libors L_i are assumed to be log-normally distributed in the t_n -forward measure, with numeraire the discount bond P_{t,t_n}

$$L_i = \tilde{L}_i \exp\left(\psi x_i - \frac{1}{2}\psi^2 t_i\right) \quad (2)$$

For simplicity we will denote the value of the Markov driver at time t_i as $x_i \equiv x(t_i)$. We assume that the

Libor volatility ψ is a constant, although a more general formulation of the model is possible, wherein ψ has term structure. For the purpose of illustrating the phenomenon considered here, it will be sufficient to consider a constant Libor volatility ψ .

The specification of the Markov-functional model considered here is somewhat different from that usually adopted in the literature [1–4], where the distribution of the forward Libors L_i in the terminal measure is determined such that the market caplet or swaption smile is correctly reproduced. Here we will assume it as given by (2), and will study its implications for the caplet smile as a function of the volatility parameter ψ . We will show that for sufficiently small ψ , the caplet log-normal implied volatility is equal to ψ to a good approximation, while for larger values of ψ the model undergoes a qualitative transition and a nontrivial caplet smile is generated. For arbitrary values of ψ the caplet smile can be represented by a finite superposition of log-normal distributions for the Libor rate in the forward measure.

The zero coupon bonds $P_{i,j}$ can be expressed as functions of the one-dimensional Markov process $x(t)$. We will denote the numeraire-rebased zero coupon bond prices as $\hat{P}_{i,j} = P_{i,j}/P_{i,n}$. They are martingales in the t_n -forward measure, and thus satisfy the condition

$$\hat{P}_{i,j} = \mathbb{E}_n\left[\frac{1}{P_{j,n}}|\mathcal{F}_i\right] \quad (3)$$

It can be shown [6, 7] that imposing the martingale condition (3) for all possible i, j pairs determines uniquely the convexity-adjusted Libors \tilde{L}_i .

A. Analytical solution

For the time-homogeneous case of a constant volatility ψ , it can be shown that the model can be solved analytically [13]. The solution can be expressed as an analytical expression for the one-step zero coupon bonds $\hat{P}_{i,i+1}$ which are given by

$$\hat{P}_{i,i+1}(x_i) = \sum_{j=0}^{n-i-1} c_j^{(i)} e^{j\psi x_i - \frac{1}{2}(j\psi)^2 t_i} \quad (4)$$

with $c_j^{(i)}$ a set of constant coefficients to be determined. The convexity-adjusted Libors are given by

$$\tilde{L}_i = \frac{\hat{P}_{0,i} - \hat{P}_{0,i+1}}{N_i \tau_i}, \quad (5)$$

$$N_i \equiv \mathbb{E}[\hat{P}_{i,i+1} e^{\psi x_i - \frac{1}{2}\psi^2 t_i}] = \sum_{j=0}^{n-i-1} c_j^{(i)} e^{j\psi^2 t_i}.$$

The coefficients $c_j^{(i)}$ satisfy the recursion relation

$$c_j^{(i)} = c_j^{(i+1)} + \tilde{L}_{i+1} \tau_{i+1} c_{j-1}^{(i+1)} e^{(j-1)\psi^2 t_{i+1}} \quad (6)$$

which must be solved simultaneously with Eq. (5) for \tilde{L}_i . The initial condition is $c_0^{(n-1)} = 1, \tilde{L}_{n-1} \tau_{n-1} = \hat{P}_{0,n-1} - 1$. The recursion relation (6) can be solved backwards in time, for all $i \leq n-1$, finding all coefficients recursively. The coefficients $c_j^{(i)}$ and the convexity-adjusted Libors \tilde{L}_i determine the solution of the model, and the zero coupon bonds $P_{i,j}$ can be expressed as functions of $x = x_i$.

The recursion relation (6) can be solved more elegantly by introducing the generating function at the time horizon t_i

$$f^{(i)}(x) \equiv \sum_{j=0}^{n-i-1} c_j^{(i)} x^j \quad (7)$$

The generating function $f^{(i)}(x)$ takes known values at $x = 0, 1$

$$f^{(i)}(0) = 1, \quad f^{(i)}(1) = \hat{P}_{0,i+1} \quad (8)$$

where the second constraint follows from a sum rule for the coefficients $c_i^{(j)}$ [13].

The generating function satisfies a recursion relation, expressing the generating function at time t_i in terms of the generating function at the next time t_{i+1}

$$f^{(i)}(x) = f^{(i+1)}(x) + \tilde{L}_{i+1} \tau_{i+1} f^{(i+1)}(x e^{\psi^2 t_{i+1}}) \quad (9)$$

The initial condition for the recursion is $f^{(n-1)}(x) = 1$. The expectation value N_i appearing in the expression for the convexity-adjusted Libor \tilde{L}_i is

$$N_i = f^{(i)}(e^{\psi^2 t_i}) \quad (10)$$

The generating function $f^{(i)}(x)$ and thus the coefficients $c_j^{(i)}$ can be found in closed form in the two limiting cases of very small and very large volatility ψ . The zero volatility limit $\psi = 0$ is

$$f_0^{(i)}(x) = \prod_{j=i+1}^{n-1} (1 + L_j^{\text{fwd}} \tau_j). \quad (11)$$

where $\tilde{L}_j = L_j^{\text{fwd}} = \tau_j^{-1}(\hat{P}_{0,j}/\hat{P}_{0,j+1} - 1)$ is the forward Libor for the time period (t_j, t_{j+1}) .

In the asymptotically large volatility limit $\psi \rightarrow \infty$, the recursion relation (9) can be solved again exactly with the result

$$f_\infty^{(i)}(x) = 1 + (\hat{P}_{0,n-1} - 1)x + (\hat{P}_{0,n-2} - \hat{P}_{0,n-1})x^2 + \dots + (\hat{P}_{0,i+1} - \hat{P}_{0,i+2})x^{n-i-1}. \quad (12)$$

The most distinctive feature of the model in the large volatility limit is a very fast increase of $N_i = f^{(i)}(e^{\psi^2 t_i})$ with the volatility, which is much faster than in the low volatility limit. This causes the convexity-adjusted Libors \tilde{L}_i to become very small. Their asymptotic expression in the large volatility phase is [13]

$$\tilde{L}_i = \frac{\hat{P}_i - \hat{P}_{i+1}}{(\hat{P}_{i+1} - \hat{P}_{i+2})\tau_i} e^{-(n-i-1)\psi^2 t_i} (1 + O(e^{-\psi^2 t_i})) \quad (13)$$

In practice \tilde{L}_i can become very small, below machine precision, which can complicate the numerical simulation of the model in the large volatility regime.

B. The Libor phase transition

The analytical solution of the model presented above can be used to study exactly its behaviour as a function of the volatility parameter ψ . It turns out that this is not smooth for all quantities of the model. Certain expectation values, such as N_i given in (5), have a dependence on ψ which has a singularity at a special value of volatility which will be called the critical volatility ψ_{cr} . This singularity is a sudden change in the derivative $dN_i/d\psi$ at the critical point, and becomes more sharp as the time step τ decreases, such that it approaches a nonanalyticity point in the continuum limit [13].

The underlying reason for this phenomenon is a singularity in the generating function $f^{(i)}(x)$ at a certain value x_* . This value is related to the position of the zeros of $f^{(i)}(x)$ in the complex plane. The generating function is a polynomial in x of degree $n - i - 1$ with positive coefficients, and thus does not have any zeros on the positive real axis. It has $n - i - 1$ zeros, which are arranged in complex conjugate pairs symmetric with respect to the real axis, along a curve surrounding the origin. The singularity point x_* is the point on the real axis which is closest to the complex zeros. At this point the derivative of the generating function has a discontinuity which is proportional to the density of the zeros around the positive real axis.

This phenomenon is similar to a first order phase transition in condensed matter physics, where the thermodynamical potentials have a discontinuity in the first derivative at the critical point [14]. The analogy becomes even closer in the Lee-Yang formalism of the phase transitions [15], where the critical point is associated with the complex zeros of the grand canonical partition function.

Returning to the Markov functional model with log-normally distributed rates, the singularity in N_i occurs at the point ψ_{cr} given by

$$e^{\psi_{\text{cr}}^2 t_i} = x_* \quad (14)$$

This determines the critical volatility ψ_{cr} . A similar phenomenon occurs for any expectation value of the form similar to N_i

$$\mathbb{E}_n[\hat{P}_{i,i+1} e^{\phi x - \frac{1}{2} \phi^2 t_i}] = f^{(i)}(e^{\psi \phi t_i}) \quad (15)$$

which can be expressed in terms of the generating function $f^{(i)}(x)$ as shown. The critical volatility corresponding to this expectation value is found in analogy to Eq. (14) and is given by $\exp(\psi \phi t_i) = x_*$.

The precise value of the critical volatility depends on the time step i , and on the entire shape of the yield curve $P_{0,i}$. We consider in the following for illustration the case of a constant short rate r_0 , which corresponds to the discount bonds $P_{0,i} = \exp(-r_0 \tau i)$. The simplest estimate of the critical volatility can be obtained from the zeros of the asymptotic generating function $f_{\infty}^{(i)}(x)$, corresponding to very large volatility. A very good approximation

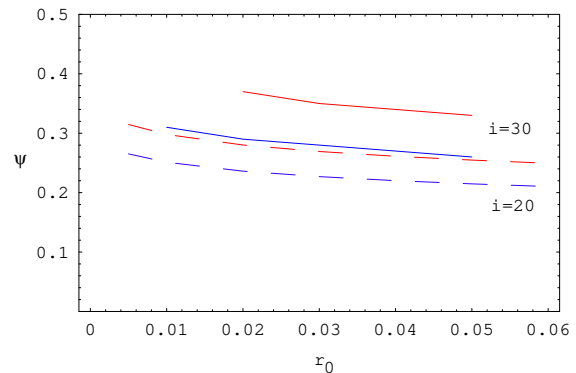


FIG. 1: The phase diagram in coordinates (r_0, ψ) of the log-normal Markov functional model with constant forward short rate. The red curves correspond to $i = 30$ (Libor rate set at $t_i = 7.5$) and the blue curves to $i = 20$ (Libor rate set at $t_i = 5$). The solid lines are exact phase boundaries, while the dashed lines correspond to the approximative result Eq. (17). The remaining model parameters are $n = 40$, $\tau = 0.25$, corresponding to a simulation with total time 10y and quarterly time steps.

for the position of these zeros can be used to obtain

$$e^{r_0 \tau + \psi_{\text{cr}}^2 t_i} = \left(\frac{1}{1 - e^{-r_0 \tau}} \right)^{1/(n-i-1)} \quad (16)$$

which can be approximated, to a good precision, as

$$\psi_{\text{cr}}^2 = \frac{1}{i(n-i-1)\tau} \log \left(\frac{1}{r_0 \tau} \right). \quad (17)$$

The relation (17) reproduces the main features of the critical volatility observed in numerical simulations:

- The critical volatility decreases as the size of the time step τ is reduced, approaching a very small value in the continuum limit.
- The critical volatility increases as the short rate r_0 is reduced, approaching a very large volatility as the rate r_0 becomes very small.

These properties can be summarized by the phase diagram of the model, shown in Fig. 1. This diagram shows the critical volatility $\psi_{\text{cr}}(r_0)$ of the model with flat forward short rate r_0 as a function of r_0 . We consider two values of $i = 20, 30$ in a simulation with $n = 40$ time steps and $\tau = 0.25$. We show both the exact critical volatility (solid lines) which can be found as the value of ψ at which $\partial_{\psi}^2 \log N_i$ is maximized, and the simple approximation (17). These curves are compared with the approximative results obtained from (17). We note that the approximative result (17) underestimates the correct value of the critical volatility by about 10%.

III. THE LIBOR DISTRIBUTION FUNCTION

By the model definition, the Libor rates L_i are log-normally distributed in the t_n -forward measure. A more natural measure for pricing instruments depending on the Libor rate L_i is the t_{i+1} -forward measure, where the numeraire is the zero-coupon bond $P_{t,i+1}$, maturing at time t_{i+1} . We will consider in the following the following two measures

$$\mathbb{P}_n : \quad \text{numeraire } P_{t,n} \quad (18)$$

$$\mathbb{P}_{i+1} : \quad \text{numeraire } P_{t,i+1} \quad (19)$$

As a concrete example, consider a caplet \mathbf{C}_i on the Libor rate $L_{i,i+1} = \tau_i^{-1}(P_{i,i+1}^{-1} - 1)$, set at time t_i and paid at time t_{i+1} . The payoff of this instrument is $(L_i - K)_+$, and its price in the t_n -forward measure \mathbb{P}_n is

$$C_i(K) = P_{0,n} \mathbb{E}_n[(L_i - K)_+ \hat{P}_{i,i+1}] \quad (20)$$

Expressed in the \mathbb{P}_{i+1} measure, the expression for the caplet price \mathbf{C}_i simplifies and is given by

$$C_i(K) = P_{0,i+1} \mathbb{E}_{i+1}[(L_i - K)_+] \quad (21)$$

The expectation value in \mathbb{P}_{i+1} measure can be expressed as an integral of the payoff convoluted with the probability distribution function of the Libor L_i in this measure. We will denote this distribution $\Phi_i(L_i)$, and we have

$$\mathbb{E}_{i+1}[(L_i - K)_+] = \int_0^\infty dL_i \Phi_i(L_i) (L_i - K)_+ \quad (22)$$

In the following we will study in some detail the distribution function $\Phi_i(x)$, and its properties. The pdf of the Libor L_i in the \mathbb{P}_{i+1} measure can be obtained by comparing Eqs. (20) and (21). It is given by

$$\Phi_i(L) = \frac{1}{\hat{P}_{0,i+1}} \frac{e^{-x_0^2/(2t_i)}}{\sqrt{2\pi t_i}} \frac{1}{\psi L} \hat{P}_{i,i+1}(x_0) \quad (23)$$

with $x_0 = x_0(L)$ determined as

$$x_0 = \frac{1}{\psi} \log \frac{L}{L_i} + \frac{1}{2} \psi t_i. \quad (24)$$

We would like to study how the Libor distribution function $\Phi_i(L)$ changes as the volatility ψ is increased from zero to large values. At zero volatility $\psi = 0$, this distribution is a delta function concentrated at the forward value

$$\Phi_i(L, \psi = 0) = \delta(L - L_i^{\text{fwd}}) \quad (25)$$

As the volatility increases, the distribution widens out. We show in Fig. 2 the shape of the distribution $\Phi_i(L)$ for several values of the volatility ψ . For moderate values of ψ , below the critical volatility ψ_{cr} , the distribution has a typical humped shape, peaked around the forward value L_i^{fwd} .

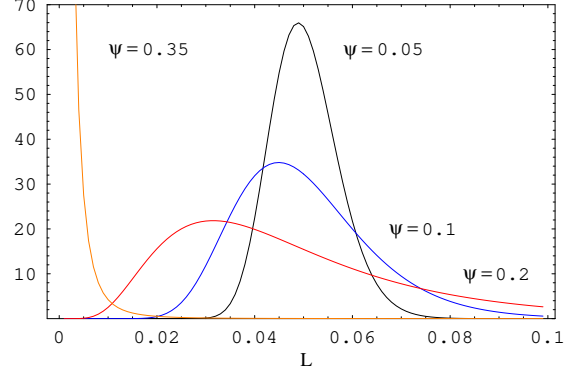


FIG. 2: The probability distribution function $\Phi_i(L)$ for the Libor L_i in the measure \mathbb{P}_{i+1} for several values of the volatility ψ . The plots correspond to a constant forward short rate $r_0 = 5\%$, which gives $L_i^{\text{fwd}} = 5.0314\%$. The remaining parameters are $i = 30$, $n = 40$, $\tau = 0.25$.

Above the critical volatility $\psi > \psi_{\text{cr}}$ the distribution function $\Phi_i(L)$ undergoes a dramatic change: its support collapses very rapidly to very small values of L . The “collapse” of the Libor distribution $\Phi_i(L)$ to very small values close to zero is another surprising phenomenon in the high-volatility phase of this model.

Naively, one may ascribe this phenomenon to the fact that the convexity-adjusted Libors \tilde{L}_i in the defining equation of the model (2) become very small in the large volatility phase. On further reflection the situation is slightly more complicated, for two reasons. First, the log-normal distribution (2) is in the terminal measure \mathbb{P}_n , while we are interested here in the distribution function in \mathbb{P}_{i+1} measure. Second, the martingale condition for L_i in \mathbb{P}_{i+1} measure requires that the average of L_i should be equal to its forward value $\mathbb{E}[L_i] = L_i^{\text{fwd}}$, which would not be possible if the distribution were concentrated near $L_i = 0$. The only way for the martingale condition to be satisfied is that the distribution has a long fat tail, which contributes significantly to the average of L .

In the following we would like to explore this phenomenon in more detail. The analysis presented next will confirm the heuristic arguments mentioned above. We start by showing that the distribution function $\Phi_i(L)$ can be represented as a sum of log-normal distributions. Define the log-normal distribution with average parameter μ and dispersion σ

$$\phi(x; \mu, \sigma) = \frac{1}{x\sqrt{2\pi}\sigma} e^{-\frac{1}{2\sigma^2}(\log x - \mu)^2} \quad (26)$$

The j -th moment of the x variable under the distribution $\phi(x; \mu, \sigma)$ is

$$\mathbb{E}[x^j] = e^{j\mu + \frac{1}{2}j^2\sigma^2} \quad (27)$$

The distribution function of the L_i Libor in the \mathbb{P}_{i+1} measure (23) can be represented as a sum of log-normal

distributions with different averages but the same variance

$$\Phi_i(L) = \frac{1}{\hat{P}_{i+1}} \sum_{j=0}^{n-i-1} c_j^{(i)} \phi(L; \mu_j^{(i)}, \sigma_i = \psi\sqrt{t_i}) \quad (28)$$

where

$$\mu_j^{(i)} = \log \left(\tilde{L}_i e^{(j-\frac{1}{2})\psi^2 t_i} \right) \quad (29)$$

The average value of L under the log-normal distribution $\phi(L; \mu_j^{(i)}, \sigma_i = \psi\sqrt{t_i})$ is

$$\mathbb{E}[L|\phi(L; \mu_j^{(i)}, \sigma_i)] = \tilde{L}_i e^{j\psi^2 t_i} \quad (30)$$

so each of these log-normal distributions is peaked at successively higher values of L . Specifically, the pdf of the Libor (28) consists of a sum of log-normal distributions with averages $\tilde{L}_i, \tilde{L}_i e^{\psi^2 t_i}, \dots, \tilde{L}_i e^{(n-i-1)\psi^2 t_i}$, and weights $1/\hat{P}_{0,i+1}, c_1^{(i)}/\hat{P}_{0,i+1}, c_2^{(i)}/\hat{P}_{0,i+1}, \dots, c_{n-i-1}^{(i)}/\hat{P}_{0,i+1}$. We recall that the weights add up to 1 due to the exact sum rule $\sum_{j=0}^{n-i-1} c_j^{(i)} = \hat{P}_{0,i+1}$.

The weights $c_j^{(i)}/\hat{P}_{0,i+1}$ of the terms with $j > 1$ decrease sufficiently fast with j , such that the total average of L is equal to the forward Libor rate, as required by the martingale condition for L_i in the \mathbb{P}_{i+1} measure

$$\begin{aligned} \mathbb{E}_{i+1}[L] &= \frac{1}{\hat{P}_{0,i+1}} \sum_{j=0}^{n-i-1} c_j^{(i)} \mathbb{E}[L|\phi(L; \mu_j^{(i)}, \sigma_i)] \quad (31) \\ &= \frac{1}{\hat{P}_{0,i+1}} \sum_{j=0}^{n-i-1} c_j^{(i)} \tilde{L}_i e^{j\psi^2 t_i} = L_i^{\text{fwd}}. \end{aligned}$$

The representation (28) of the distribution function can be used to obtain a qualitative understanding of the behaviour of this distribution function in the large volatility limit $\psi^2 t_i \gg 1$. In this limit the asymptotic behaviour of the convexity adjusted Libors \tilde{L}_i is given by (13). In the large volatility regime, the convexity adjusted Libors decrease very rapidly with the volatility ψ . This means that most of the log-normal components of the distribution function $\Phi_i(L)$ have vanishingly small averages, except for the last one with $j = n - i - 1$

$$\mathbb{E}[L|\phi(L; \mu_j^{(i)}, \sigma_i)] = L_i^{\text{max}} e^{-(n-i-1-j)\psi^2 t_i}, \quad (32)$$

where

$$L_i^{\text{max}} = \frac{\hat{P}_i - \hat{P}_{i+1}}{(\hat{P}_{i+1} - \hat{P}_{i+2})\tau_i} = L_i^{\text{fwd}} \frac{1 + L_{i+1}^{\text{fwd}}\tau_{i+1}}{L_{i+1}^{\text{fwd}}\tau_{i+1}}. \quad (33)$$

For typical values of model parameters, such as $L^{\text{fwd}} = 5\%$, $\tau = 0.25$, one has $L^{\text{max}} \sim 500\%$ which is a very large value compared to typical rates.

In the large volatility regime the coefficients $c_j^{(i)}$ are all comparable, such that the shape of the distribution

function $\Phi_i(L)$ is expected to be very concentrated near $L = 0$, corresponding to the terms with $j = 0, 1, \dots, n - i - 2$, and to have a fat tail extending to very large values of $L \sim L^{\text{max}}$, corresponding to the term with $j = n - i - 1$. This is confirmed by direct calculation of the distribution function in the large volatility limit, as observed in Fig. 2.

The behaviour of the Libor distribution function in \mathbb{P}_{i+1} measure in the large volatility limit is related to a numerical issue discussed in [13], which is responsible for the unobservability of the phase transition in usual simulation methods such as Monte Carlo or finite difference methods. This numerical issue appears in the calculation of the expectation value (5) as an integral

$$\begin{aligned} N_i &= \mathbb{E}[\hat{P}_{i,i+1} e^{\psi x - \frac{1}{2}\psi^2 t_i}] \quad (34) \\ &= \int_{-\infty}^{\infty} \frac{dx}{\sqrt{2\pi t_i}} e^{-\frac{x^2}{2t_i}} \hat{P}_{i,i+1}(x) e^{\psi x - \frac{1}{2}\psi^2 t_i}. \end{aligned}$$

At volatilities above the critical value $\psi > \psi_{\text{cr}}$ the integrand in this expression develops a secondary peak at a relatively large value of $|x| \sim 10\sqrt{t_i}$, in addition to the peak around $x \sim 0$. The secondary peak gives the dominant contribution to the integral in the large volatility limit. However, the region of large x where it appears is very poorly sampled in usual simulation methods, which thus will fail to take it into account.

The numerical significance of the secondary peak can be better understood by changing variables in the integral (34) from x to L_i , the Libor rate. We observe that the integrand of (34) is simply related to the Libor distribution function $\Phi_i(L)$ in the \mathbb{P}_{i+1} measure, when expressed in terms of $x = x(L)$ given in Eq. (24). The integral in (34) becomes, after changing the integration variable from x to L

$$N_i = \hat{P}_{0,i+1} \int_0^{\infty} dL \Phi_i(L) \frac{L}{\tilde{L}_i}. \quad (35)$$

The secondary peak in the integrand of (34) becomes the fat tail of $\Phi_i(L)$, while the peak near $x \sim 0$ corresponds to the region of $L \sim \tilde{L}_i$. As discussed above, the fat tail of $\Phi_i(L)$ is essential in order for the integral above to reproduce correctly its non-arbitrage value; the counterpart of this statement in the x -integral (34) is that the secondary peak is also required by the consistency of the model, and can not be neglected.

A. The moments of the Libor distribution function

In this section we study the moments of the Libor distribution function $\Phi_i(L)$ in the \mathbb{P}_{i+1} measure. We will show that its moments, and thus its characteristic function

$$\tilde{\Phi}_i(t) = \int_{-\infty}^{\infty} dL e^{itL} \Phi_i(L) = \sum_{j=0}^{\infty} \frac{(it)^j}{j!} \mathbb{E}[L^j] \quad (36)$$

can be expressed in terms of the generating function $f^{(i)}(x)$. When considered as functions of the volatility

ψ , the n -th moment of the distribution function $M_n = \mathbb{E}[L_i^n]$ is nonanalytic at $\psi_{\text{cr}}^{(n)}$, related to the nonanalyticity point of the generating function x_* as $x_* = e^{n\psi_{\text{cr}}^2 t_i}$.

The moments of $\Phi_i(L)$ can be computed straightforwardly, and can be expressed in terms of the generating function $f^{(i)}(x)$ as follows

$$M_j = \mathbb{E}_{i+1}[L_i^j] = \int_0^\infty dL_i (L_i)^j \Phi_i(L_i) \quad (37)$$

$$= \frac{1}{\hat{P}_{0,i+1}} \tilde{L}_i^j e^{\frac{1}{2}j(j-1)\psi^2 t_i} f^{(i)}(e^{j\psi^2 t_i}).$$

We consider a few particular cases of the relation Eq. (37). The first two moments $j = 0, 1$ do not contain dynamical information, and are constrained by general considerations as follows. The $j = 0$ moment is the normalization integral, and is indeed equal to 1 by the condition (8)

$$M_0 = \frac{1}{\hat{P}_{0,i+1}} f^{(i)}(1) = 1. \quad (38)$$

The first moment can be found again in closed form, and is equal to the forward Libor rate L_i^{fwd} , as expected

$$M_1 = \frac{1}{\hat{P}_{0,i+1}} \tilde{L}_i f^{(i)}(e^{\psi^2 t_i}) = \frac{\hat{P}_{0,i} - \hat{P}_{0,i+1}}{\hat{P}_{0,i+1} \tau_i} = L_i^{\text{fwd}}. \quad (39)$$

This expresses the martingale condition for L_i in the \mathbb{P}_{i+1} measure.

More interesting is the result for the second moment M_2 . This determines the equivalent lognormal volatility of the Libor rate L_i as

$$\sigma_{\text{LN}}^2 t_i = \log\left(\frac{M_2}{M_1^2}\right) = \log\left(\hat{P}_{0,i+1} e^{\psi^2 t_i} \frac{f^{(i)}(e^{2\psi^2 t_i})}{[f^{(i)}(e^{\psi^2 t_i})]^2}\right) \quad (40)$$

In the small volatility limit $\psi^2 t_i \ll 1$ the equivalent lognormal volatility can be computed with the help of (11), and is approximatively equal to the volatility parameter ψ

$$\sigma_{\text{LN}}^2 = \psi^2 (1 + O(\psi^2 t_i)). \quad (41)$$

This shows that in the small volatility limit all caplet volatilities (for all i) are approximately equal to ψ .

When considered as a function of the volatility ψ , the moments $M_j, j \geq 2$ of the Libor distribution function $\Phi_i(L)$ have non-analytic dependence on ψ at a value of the volatility $\psi_{\text{cr}}^{(j)}$ given by the solution to the equation

$$x_*(\psi) = e^{j\psi^2 t_i} \quad (42)$$

where $x_*(\psi)$ is the non-analyticity of the generating function $f^{(i)}(x)$ at time horizon t_i . In general the position of the non-analyticity point depends on the volatility parameter ψ . The value of $x_*(\psi)$ converges to a well-defined value in the very large volatility limit $\psi \rightarrow \infty$. In this limit, $x_*(\psi)$ is given by the point on the real

axis where the complex zeros of the asymptotic generating function $f_\infty^{(i)}(x)$ pinch the real axis. This function is given in Eq. (12). In [13] we studied in detail the zeros and the non-analyticity point of the large volatility asymptotic generating function $f_\infty^{(i)}(x)$ for the case of a constant forward short rate. For this case one obtains the result (16) for the critical volatility.

In the asymptotic limit of a very large volatility, the position of the non-analyticity point x_* does not depend on ψ , such that the critical volatility of the moments of the Libor distribution function are all related as

$$\psi_{\text{cr}}^{(j)} = \frac{\psi_{\text{cr}}}{\sqrt{j}}, \quad \psi \rightarrow \infty \quad (43)$$

However, for generic cases, the non-analyticity point occurs at moderate values of the volatility ψ , and its position depends on ψ as shown in (42).

We illustrate the non-analyticity in volatility of the moments M_j on the example of the second moment M_2 . This is the most important moment from a practical point of view, as it determines the Black log-normal caplet volatility according to Eq. (40). In Figure 4 we show a plot of equivalent Black caplet volatility σ_{LN} as a function of ψ (red curve) at the time horizon $i = 30$ in a simulation with $n = 40$ quarterly time steps.

The equivalent log-normal volatility σ_{LN} has two turning points, at ψ around 0.3 and at 0.33. The critical point at the time horizon considered here is $\psi_{\text{cr}} = 0.33$, which corresponds to the second point. In order to understand the first turning point, we show in the Appendix the zeros of the generating function $f^{(i)}(x)$ together with two circles of radius $e^{\psi^2 t_i}$ and $e^{2\psi^2 t_i}$. From these plots one can see that the first turning point coincides with the zeros crossing the larger circle of radius $e^{2\psi^2 t_i}$, and the second turning point corresponds to the volatility ψ at which the zeros cross the smaller circle, of radius $e^{\psi^2 t_i}$. Since the position of the zeros changes with ψ , the first turning point (the critical volatility of the second moment M_2) $\psi_{\text{cr}}^{(2)} = 0.3$ differs from the large volatility limit prediction $\psi_{\text{cr}}/\sqrt{2} \simeq 0.23$, obtained by assuming stationary zeros.

Only the first few moments have non-analyticity points. The reason for this is that at very low volatilities ψ , the zeros of the generating function do not surround the origin, but a gap is present between the real axis and the zeros. As the volatility increases the zeros move closer to the origin, and close together on the real axis. However, at this point they have crossed already the circles of radii $e^{j\psi^2 t_i}$, with $j > j_0$ such that the moments M_j do not have a non-analyticity point for sufficiently large $j > j_0$. The maximal index j_0 of the moment of the Libor pdf L_i which still has a phase transition depends on the time horizon t_i considered.

The price of an instrument which is sensitive to the j -th moment will have a nonanalyticity point at the corresponding value of the volatility. For the second moment this is the case for example with the Libor payment in arrears, discussed in the next section.

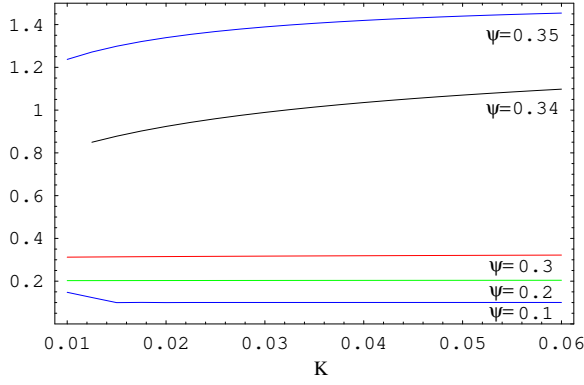


FIG. 3: Implied caplet volatility smile for several values of the volatility ψ , as function of the strike K . The caplet is defined on the rate L_{30} in a simulation with $n = 40$ time steps, $\tau = 0.25$ and constant forward short rate $r_0 = 5\%$. The forward Libor is $L_i^{\text{fwd}} = 5.0314\%$.

B. Caplet pricing

A closed form expression for the caplet price can be found by direct evaluation of the expectation value in (20)

$$C_i(K) = P_{0,n} \sum_{j=0}^{n-i-1} c_j^{(i)} [\tilde{L}_i e^{j\psi^2 t_i} N(f_1) - KN(f_2)] \quad (44)$$

with

$$f_1 = -\frac{1}{\sqrt{t_i}} [x_0(K) - (j+1)\psi t_i] \quad (45)$$

$$f_2 = -\frac{1}{\sqrt{t_i}} [x_0(K) - j\psi t_i] \quad (46)$$

$$x_0(K) = \frac{1}{\psi} \log \frac{K}{\tilde{L}_i} + \frac{1}{2} \psi t_i. \quad (47)$$

This has the typical form of a mixing solution [16, 17] for an option price on an asset with a probability distribution consisting of a superposition of log-normal distributions.

Figure 3 shows typical results for the log-normal caplet smile for several values of the volatility ψ , obtained from the exact formula (44). At low values of ψ the volatility is independent of strike, which means that the distribution $\Phi_i(L)$ is approximately log-normal. In Figure 4 we show a plot of the exact caplet volatility for ATM strike $K = 5\%$, from which one can see that, for small ψ , the ATM volatility is to a very good approximation equal to ψ . This agrees with the prediction (40).

At larger values of ψ above the critical volatility $\psi_{\text{cr}} = 0.33$, the smile is not flat, which signals deviations from a log-normal distribution for $\Phi_i(L)$.

An approximation for the caplet prices can be obtained by using the equivalent log-normal caplet volatility (40) into the Black-Scholes formula

$$C_i^{\text{app}}(K) = P_{0,i+1} [L_i^{\text{fwd}} N(d_1) - KN(d_2)] \quad (48)$$

with $d_{1,2} = \frac{1}{\sigma_{\text{LN}} \sqrt{t_i}} [\log(K/L_i^{\text{fwd}}) \pm \frac{1}{2} \sigma_{\text{LN}}^2 t_i]$.

In Figure 4 we show also a plot (red curve) of the equivalent Black caplet volatility from (40), comparing it with the exact caplet volatility (black curve). The critical volatility corresponding to the caplet shown in this plot is $\psi_{\text{cr}} = 0.33$. We observe that the exact and approximative volatilities agree with each other for small ψ , where they satisfy very well the proportionality relation (41). This region is the intended region of applicability of the model in practice.

At larger values of ψ a sharp turn in the equivalent volatility occurs at $\psi \sim 0.3$, which corresponds to the critical volatility of the second moment of the Libor distribution function, as explained in the previous section. The second turn point is at $\psi_{\text{cr}} = 0.33$ which is the critical volatility of the model. It is interesting that for $\psi > \psi_{\text{cr}}$ the equivalent log-normal volatility decreases while the model volatility ψ increases.

The exact ATM caplet volatility has a first turning point which is closer to the critical value of the volatility. The disagreement between the exact ATM and the equivalent log-normal volatilities implies that the Libor distribution function deviates appreciably from a log-normal shape for values of ψ close to the critical volatility. The fast increase in the ATM caplet volatility above the critical volatility is explained by the appearance of the long tail of the Libor distribution function $\Phi_i(L)$ extending to very large values of L . This gives a large contribution to the caplet price, which is given by a simple integral over $\Phi_i(L)$

$$C_i(K) = P_{0,i+1} \int_0^\infty dL (L - K)_+ \Phi_i(L) \quad (49)$$

We remarked on the numerical importance of the tail of the $\Phi_i(L)$ distribution in relation to the integral (35), where it is needed in order for this integral to reproduce its non-arbitrage value. It is thus expected that the tail of this distribution will contribute significantly also to the price of the caplet $C_i(K)$ above the critical point.

IV. LIBOR PAYMENT IN ARREARS

Similar non-analyticity effects will appear when pricing other interest rates derivatives as well. We illustrate this on the example of the Libor payment in arrears. This instrument pays $L_i \tau_i$ at time t_i , where L_i is the Libor rate for the (t_i, t_{i+1}) period, set at t_i . The price of this instrument in the terminal measure is

$$\begin{aligned} A_i &= P_{0,n} E_n [L_i(x_i) \tau_i P_{i,n}^{-1}(x_i)] \\ &= P_{0,n} E_n [L_i(x_i) \tau_i \hat{P}_{i,i+1}(x_i) (1 + L_i(x_i) \tau_i)]. \end{aligned} \quad (50)$$

The first term, linear in L_i , is known exactly from the pricing of a forward-rate agreement (FRA)

$$E_n [L_i(x_i) \tau_i \hat{P}_{i,i+1}(x_i)] = \hat{P}_{0,i} - \hat{P}_{0,i+1} \quad (51)$$

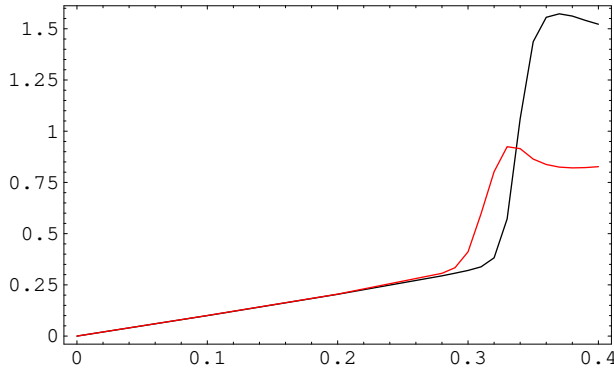


FIG. 4: The exact ATM caplet volatility (black), and the equivalent log-normal caplet volatility σ_{LN} computed using (40) (red), as functions of the volatility parameter ψ . The caplet strike is $K = 5\%$, the forward Libor is $L^{\text{fwd}} = 5.0314\%$, corresponding to a constant forward short rate $r_0 = 5\%$. The remaining model parameters are $i = 30$, $n = 40$, $\tau = 0.25$.

$$= P_{0,i+1}(L_i^{\text{fwd}}\tau_i).$$

The only non-trivial part is the pricing of the term quadratic in L_i , which can be expressed in terms of the generating function

$$E_n[L_i^2(x_i)\hat{P}_{i,i+1}(x_i)] = \tilde{L}_i^2 e^{\psi^2 t_i} f^{(i)}(e^{2\psi^2 t_i}) \quad (52)$$

Recall that the convexity-adjusted Libor is given by

$$\tilde{L}_i = \frac{\hat{P}_{0,i} - \hat{P}_{0,i+1}}{f^{(i)}(e^{\psi^2 t_i})\tau_i} = \hat{P}_{0,i+1} L_i^{\text{fwd}} \frac{1}{f^{(i)}(e^{\psi^2 t_i})} \quad (53)$$

Combining all the pieces together we get for the price of a Libor payment in arrears

$$\frac{A_i}{P_{0,i+1}} = (L_i^{\text{fwd}}\tau_i) + \hat{P}_{0,i+1}(L_i^{\text{fwd}}\tau_i)^2 e^{\psi^2 t_i} \frac{f^{(i)}(e^{2\psi^2 t_i})}{[f^{(i)}(e^{\psi^2 t_i})]^2} \quad (54)$$

The second term is the convexity adjustment, and can be expressed in terms of the equivalent log-normal volatility σ_{LN} introduced in (40). We obtain the following result for the price of a Libor payment in arrears in the model with log-normally distributed Libors in the terminal measure

$$A_i = P_{0,i+1}(L_i^{\text{fwd}}\tau_i) \left\{ 1 + (L_i^{\text{fwd}}\tau_i) e^{\sigma_{\text{LN}}^2 t_i} \right\} \quad (55)$$

This can be compared with the exact result for the price of a Libor payment in arrears in a model with exact log-normal caplet volatility ψ for the Libor L_i

$$A_i = P_{0,i+1}(L_i^{\text{fwd}}\tau_i) \left\{ 1 + (L_i^{\text{fwd}}\tau_i) e^{\psi^2 t_i} \right\} \quad (56)$$

This model has a log-normal Libor distribution function in the measure \mathbb{P}_{i+1} . The result (56) is identical with the

price in the model with log-normal Libor in the terminal measure \mathbb{P}_n (55), up to the replacement $\sigma_{\text{LN}} \rightarrow \psi$.

For small volatility ψ , the equivalent volatility σ_{LN} is approximatively equal to ψ , see Eq. (41). For larger volatility ψ it has a more complex behaviour as discussed in Sec.3.A, including two non-analyticity points at $\psi_{\text{cr}}^{(2)}$ and $\psi = \psi_{\text{cr}}$, as observed in Fig. 4. This means that the price of this instrument has the same non-analytical behaviour as σ_{LN} as function of ψ .

Similar non-analyticity effects can be expected to appear when pricing other interest rates derivatives, and are introduced either through non-analytic behaviour in the convexity-adjusted Libors \tilde{L}_i , or through the moments of the Libor distribution function in the \mathbb{P}_{i+1} measure. Thus non-analyticity effects appear to be a generic feature of this model.

V. CONCLUSIONS

We continued in this paper the study started in [13] of a Markov functional model with discrete log-normally distributed rates in the forward measure. This study made use of an exact solution of the model which can be obtained in the time-homogeneous limit of constant volatility. The exact solution displays non-analytic behaviour in the volatility for certain expectation values, which occurs at a critical value of the volatility. The values of the critical volatility in simulations with 10-30y and interest rates around 5% are comparable with actual log-normal caplet volatilities observed in the market, such that the existence of this phase transition is of more than academic relevance.

In this paper we studied the implications of the phase transition for the pricing of interest rates derivatives in this model. We focused on the probability distribution of the Libor rates in a natural measure, where it is simply related to the caplet pricing. We showed that the shape of this distribution function undergoes a dramatic change around the critical volatility. In the large volatility regime its defining features are a support around small Libor values, and a long fat tail. Furthermore, the moments of this distribution function have also non-analyticity points as functions of the volatility, which are related to the critical volatility. These results have implications for derivative pricing, and we considered as concrete examples caplets on Libor rates and Libor payments in arrears. The caplet prices and their volatilities display also singularities as function of the model volatility. One can expect that this phenomenon occurs also for other interest rate derivatives, and is a general feature of the Markov functional model with log-normally distributed rates in the terminal measure.

The model considered here assumes that the spot Libors are log-normally distributed in the terminal measure. This is different from the original proposed form of the Markov functional models [1–3], where this distribution is chosen such that the market caplet smile is

exactly reproduced. For reasons of practical convenience the simpler implementation of these models considered here is sometimes used, wherein the functional dependence is constrained to have a specific form, e.g. log-normal. Such models can not aim to reproduce the entire caplet smile, but only the implied caplet volatility at one particular strike for each maturity, e.g. the ATM implied volatility. The results of this paper show that at low volatilities a log-normal caplet smile can be well reproduced by assuming Libor log-normality in the terminal measure; however at larger volatility this property is not preserved, and a nontrivial cap smile is generated. In general such models will have discontinuous behaviour manifested as a phase transition, which has to be either taken into account, or avoided by appropriate limits of the model parameters.

As discussed in [13], usual implementations of this model using Monte Carlo or finite difference methods do not capture correctly the behaviour of the model in the large volatility phase, and thus the phase transition is not visible under these simulation methods. In practice one can take the view that the discretized version of the model with its built-in limitations (e.g. limits on the range of the Markovian driver x_t) is the model. The existence of the phase transition is practically relevant in this case if part of the calibration of the model is performed analytically, but then the simulation of the model is done numerically. This could lead to inconsistencies, and special care has to be used in such situations.

Finally, the arguments of this paper are limited to the time-homogeneous setting of a constant volatility, but it is entirely plausible that a very similar phenomenon will occur also in the practically relevant but analytically more complex case of time-dependent volatility $\psi(t_i)$.

Appendix

We illustrate in this Appendix the relation between the position of the zeros of the generating function $f^{(i)}(x)$ and the non-analyticity properties of the moments of the Libor distribution function discussed in Sec. 3.A. We take as a concrete example a simulation with $n = 40$ quarterly time steps, with constant forward short rate $r_0 = 5\%$, and we examine the zeros of the $f^{(i)}(x)$ at the time step $i = 30$.

The plots in Fig. 5 show the movement of the zeros of

$f^{(30)}(x)$ as a function of the volatility ψ for $\psi = 0.3 - 0.33$. On the same plots are shown also two circles with radii $e^{\psi^2 t_i}$ and $e^{2\psi^2 t_i}$. The values of the volatility at which the zeros cross these circles are the critical volatility ψ_{cr} and the critical volatility of the second moment $\psi_{cr}^{(2)}$, respectively. These critical volatilities are visible as turning points in the plot of the equivalent log-normal volatility σ_{LN} as function of ψ in Fig. 4.

A similar picture holds for the higher moments. For example, the j -th moment of the Libor distribution function $M_j = \mathbb{E}[L_i^j]$ will have a non-analyticity point at $\psi_{cr}^{(j)}$. This corresponds to that value of the volatility where the zeros of $f^{(i)}(x)$ cross the circle of radius $e^{j\psi^2 t_i}$. As mentioned in the text, for sufficiently large moments the zeros do not surround completely the origin, and these moments will not have a phase transitions.

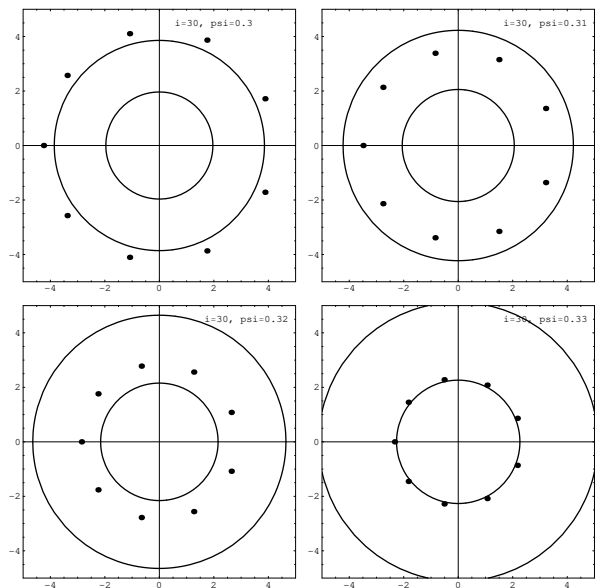


FIG. 5: The position of the zeros of the generating function $f^{(i)}(x)$ for several values of the volatility $\psi = 0.3 - 0.34$ at the time horizon $i = 30$ in a simulation with $n = 40$ quarterly time steps ($\tau = 0.25$). The two circles shown have radii $e^{\psi^2 t_i}$ and $e^{2\psi^2 t_i}$. The zeros cross these circles at ψ_{cr} and $\psi_{cr}^{(2)}$, corresponding to the critical volatility of the model, and to the critical volatility of the second moment of the Libor distribution function, respectively.

-
- [1] P. Hunt, J. Kennedy and A. Pellser, Markov-Functional Interest Rate Models, *Finance and Stochastics*, 4, 391-408 (2000).
 - [2] J. B. Hunt and J. E. Kennedy, Financial Derivatives in Theory and Practice, Wiley Series in Probability and Statistics, 2005.
 - [3] P. Balland and L. P. Hughston, Markov Market Model

Consistent with Cap Smile, *Int. J. Th. Appl. Finance*, 3, 161-181 (2000).

- [4] L. Andersen and V. Piterbarg, Interest Rate Modeling, Atlantic Financial Press, 2010.
- [5] A. Brace, D. Gatarek and M. Musiela, The market model of interest rate dynamics, *Math. Finance* 7, 125-155 (1997).

- [6] F. Jamshidian, Libor and swap markets models and measures, *Finance and Stochastics* 1, 293-330 (1997).
- [7] M. Musiela and M. Rutkowski, Martingale methods in financial modeling, Springer-Verlag (1997).
- [8] P. Glasserman and X. Zhao, Arbitrage free discretization of log-normal forward Libor and swap rate models, *Finance and Stochastics* 4, 35-68 (2000)
- [9] K. Miltersen, L. Sandmann and D. Sondermann, Closed Form Solutions for Term Structure Derivatives with Log-normal Interest Rates, *J. Finance* 52, 409-430 (1997).
- [10] L. U. Dothan, On the Term Structure of Interest Rates, *Journal of Financial Economics* 6, 59-69 (1978).
- [11] F. Black, E. Derman and W. Toy, A One-Factor Model of Interest Rates and Its Application to Treasury Bond Options, *Financial Analysts Journal* 24-32 (1990).
- [12] D. Brigo and F. Mercurio, Interest Rate Models - Theory and Practice: With Smile, Inflation and Credit, Springer Verlag 2006.
- [13] D. Pirjol, Phase Transition in a Log-normal Markov Functional Model, *J. Math. Phys.* 52, 013301 (2011), arXiv:1007.0691.
- [14] E. H. Stanley, Introduction to Phase Transitions and Critical Phenomena, Oxford University Press, 1987.
- [15] T. D. Lee and C. N. Yang, Statistical Theory of Equations of State and Phase Transitions. II. Lattice Gas and Ising Model, *Physical Review Letters* 87, 410-419 (1952); *Phys. Rev.* 87, 410 (1952).
- [16] A. L. Lewis, Option Valuation under Stochastic Volatility: with Mathematica Code, Finance Press, Newport Beach, 2000.
- [17] A. L. Lewis, The Mixing Approach to Stochastic Volatility and Jump Models, 2002.